Tuning the electronic properties of dppz-ligands and their palladium(II) complexes†

Katharina Butsch,[a] Ronald Gust,[b] Axel Klein,*[a] Ingo Ott[c] and Marco Romanski[a]

Received 11th December 2009, Accepted 1st March 2010
First published as an Advance Article on the web 25th March 2010
DOI: 10.1039/b926233d

New organometallic palladium complexes of the general type $[(RR'dppz)Pd(Me)L]^{n+}$ (RR′dppz = derivatives of dipyrido[3,2-*a*:2′,3′-*c*]phenazine with RR′ = 11-Cl, 11,12-Cl_2, 11-CF_3, 11-NO_2, 11-NH_2; L = Cl, 1-methyluracilate ($n = 0$), pyridine, cytosine, caffeine, or 1-methylcytosine, (all $n = 1$) were characterised and studied in detail by electrochemical and spectroscopic (NMR, UV/Vis-absorption and emission) methods. EPR spectroscopy and density functional calculations reveal markedly tuneable lowest unoccupied molecular orbitals (LUMO) located at the dppz ligands. Cytotoxicity experiments on HT-29 colon carcinoma and MCF-7 breast cancer cell lines show promising activities for selected compounds.

Introduction

Recently there has been much interest in the analysis and application of transition metal complexes bearing the dipyrido[3,2-*a*:2,3-*c*]phenazine (dppz) ligand. The heterocyclic π system of dppz combines the chelating function of α-diimines ("polypyridines") such as 2,2′-bipyridine (bpy), or 1,10-phenanthroline (phen)[1] with the electron and proton transfer capacity of 1,4-diazines (pyrazines, quinoxalines, phenazines, *etc.*) (Scheme 1).[2]

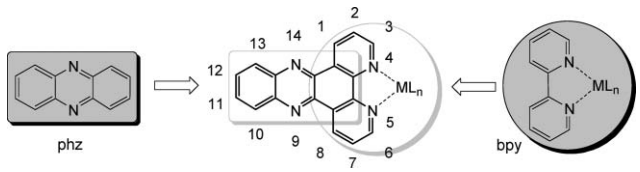

Scheme 1 The dppz-ligand, shown as a schematic transition metal complex, consists of a chelating α-diimine (bpy) part and a strongly electron-accepting phenazine (phz) part; ML_n = transition metal and *n* co-ligands.

It has been established for a number of complexes that such systems can be used as "molecular light switches"[3] (*e.g.* $[(dppz)Ru(bpy)_2]^{2+}$)[4] and as catalysts.[5] They owe this application to the planar dppz part of such complexes allowing intercalation into DNA,[6] which is the reason for the cytotoxic properties of many of these complexes. The vast majority of dppz-complexes studied so far contain Ru^{II},[4,7,8] Os^{II},[8,9] Re^{I},[8,10] Mo^{0},[8] Co^{III},[11] Ni^{II},[12] or Pt^{II},[8,13] and Cu^{I},[8,10c] while only a few Pd^{II} compounds such as [(11-Rdppz)Pd(Me)(MeCN)][BArF], (R = NO_2, COOH, Cl, H, CH_3, or NH_2),[5] $[(dppz)Pd(en)]Cl_2$ (en = ethylendiamine),[14] $[(dppz)_2Pd][BF_4]_2$ and $[(dppz)_2Pd][PF_6]_2$,[15] were reported. However, for these Pd^{II} complexes neither their "light switch" nor their cytotoxic properties were investigated. Instead, the latter complexes are used as catalysts for the CO/styrole-polymerisation.[15] Related Pt^{II} complexes $[(dppz)Pt(tN\wedge C)]CF_3SO_3$ ($tN\wedge C$ = 4-*tert*-butyl-2-phenylpyridine) and $[(dppz)Pt(L)_2](CF_3SO_3)_2$ (L = 1-methylimidazole or 4-aminopyridine) have been reported to effectively bind to double-stranded DNA and the cytotoxicity of $[(dppz)Pt\ (tN\wedge C)]CF_3SO_3$ against human carcinoma KB-3-1 and its multidrug-resistant subclone KB-V1 cell lines, was found to be 10 and 40 times higher, respectively, than cisplatin.[13]

Detailed studies have revealed that the dppz ligand has three close lying lowest unoccupied molecular orbitals (LUMO) which determine largely the electrochemical and photophysical properties. The α-diimine acceptor orbitals $b_1(\psi)$ and $a_2(\chi)$ lie above the phenazine-based π* MO, b_1(phz) and the two parts are electronically rather separated.[8] These orbitals can be influenced through various modification strategies. i) Coordination of dppz usually lowers the α-diimine-centred LUMOs, in the case of strongly electrophilic metal ions the levels might even cross.[8] This effect can be finely tuned through variation of the co-ligands on the metal and, of course, by changing the redox state of the metal.[16-18] ii) Protonation and solvation effects mainly affect the phenazine part, in both cases the N9 and N14 atoms are the main targets.[17,19] iii) Modification of the dppz-ligand by substitution of H or C atoms as well as prolongation of the π-systems is also feasible.[20-24] A great diversity of substituted dppz-ligands is already known, some of them have markedly different electrochemical and optical properties,[22] which opens various possibilities for application *e.g.* the 3,6-dibutyl substituted benzodipyridophenazines can be used as ion sensing materials[23] while complexes of Ru^{II} with phenazine-substituted ligands such as 12-NO_2-dppz

[a]*Universität zu Köln, Institut für Anorganische Chemie, Greinstraße 6, D-50969, Köln, Germany. E-mail: axel.klein@uni-koeln.de*
[b]*Institut für Pharmazie, Pharmazeutische Chemie, Freie Universität Berlin, Königin-Luise-Strasse 2+4, D-14195, Berlin, Germany*
[c]*Institute of Pharmaceutical Chemistry, Technische Universität Braunschweig, Beethovenstrasse 55, D-38106, Braunschweig, Germany*

† Electronic supplementary information (ESI) available: Further figures with absorption-, excitation- and emission spectra of free ligands and complexes and drawings of the calculated LUMOs of cdppz, dcdppz and tfmdppz can be viewed. Also, a table summarising short H···F contacts in the crystal structure of $[(dppz)Pd(Me)(Py)][SbF_6]$, and tables listing absorption, emission and electrochemical data of free ligands and complexes are provided. CCDC reference number 750425. For ESI and crystallographic data in CIF or other electronic format see DOI: 10.1039/b926233d

and 12-Cl-dppz are known to catalyse the water gas shift reaction.[24]

Furthermore, it can be expected that the substituents influence the intercalating properties and therefore the compound's toxicity. Till now this was mainly investigated using dppz-compounds with an extended aromatic system[25] and water-soluble ionic dppz analogues (with an ethyl-bridge between N4 and N5).[26] Recent investigations on Ir^{III} complexes bearing alkynyl-dppz derivatives as ligands can trigger the oxidation and reduction of DNA bases.[27]

In this work we present a series of new organopalladium complexes $[(dppz)Pd(Me)L]^{n+}$ with various dppz ligands (RR′dppz) and co-ligands of biological relevance as Cl, 1-methyluracilato ($n = 0$), pyridine, cytosine, caffeine, or 1-methylcytosine ($n = 1$) (Scheme 2). The objectives of this study were manifold. First, we wanted to explore the resulting electronic properties upon substitution at the 11 and 12 position of the dppz ligand. Secondly, fine-tuning of the electronic properties was sought by varying the complex fragments $[Pd^{II}(Me)L]$ (L = anionic ligands as chlorido or uracilato) or $[Pd^{II}(Me)L]^{+}$ (L = various neutral N-donor ligands) and co-ligands. Finally the antiproliferative properties of representative compounds were investigated to establish if these compounds exhibit cell toxicity potentially useful for anticancer treatment.

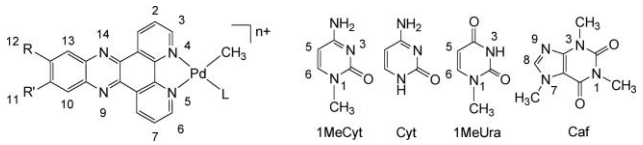

Scheme 2 Target complexes $[(RR'dppz)Pd(Me)L]^{n+}$ with partial numbering; L = pyridine, 1-methylcytosine (1MeCyt), cytosine (Cyt), caffeine = 1,3,7-trimethylxanthine (Caf), (all $n = 1$) or 1MeUra = 1-methyluracilato ($n = 0$). R, R′ = H, Cl, CF_3, NO_2, NH_2.

Results and discussion

Preparation of the RR′dppz ligands

The α-diimine ligand dppz and its derivatives were prepared by a Schiff-base condensation of pdo (1,10-phenanthroline-5,6-dione) and substituted *o*-phenylene diamines in ethanol and were isolated in excellent yields. An exception is the amino-substituted dppz, which had to be synthesised from the nitro-derivative by reduction using Pd/C in H_2-atmosphere.[28] The resulting dppz-derivatives are sparingly soluble and can therefore be separated by precipitation in good yield and purity. Some of the herein presented dppz derivatives have already been synthesised in the same way, such as ndppz[28] (R = H, R′ = NO_2) and adppz (R = H, R′ = NH_2), while cdppz (R = H, R′ = Cl) and dcdppz (R = Cl, R′ = Cl) have been reported in the form of rhenium complexes which have been synthesised from the corresponding pdo complexes and 1-Cl- or 1,2-Cl_2-phenylene-4,5-diamine.[29] The ligand tfmdppz (R = H, R′ = CF_3) is reported herein for the first time.

Preparation of the palladium complexes

Two different preparative routes (see Scheme 3) to prepare the target Pd^{II} complexes $[(RR'dppz)Pd(Me)L]^{n+}$ were compared. In both cases starting from readily available [(COD)Pd(Me)Cl].[30] The

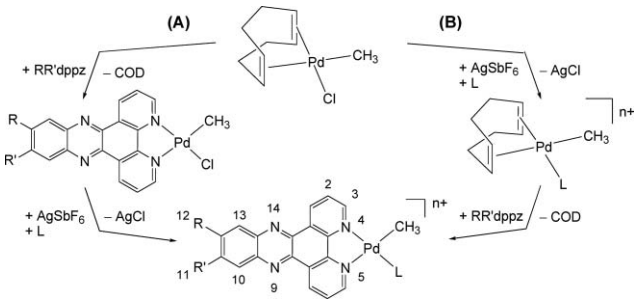

Scheme 3 Two different synthetic routes (A) and (B) for the synthesis of $[(RR'dppz)Pd(Me)L]^{n+}$ with partial numbering; COD = 1,5-Cyclooctadiene, L = various N-donor ligands.

synthesis can either be performed [route (A)] by exchanging the COD ligand by RR′dppz prior to abstraction of the chlorido ligand and introduction of the N-donor ligand. Route B starts with the chlorido-to-N-ligand exchange, followed by the replacement of the COD ligand. The first part of route B to the COD-complexes $[(COD)Pd(Me)L]^{n+}$ has been recently described.[31] Both routes have their advantages and drawbacks. The main characteristic of route A is the virtual insolubility of the chlorido complexes obtained in the first step. As a consequence the products could hardly be characterised in solution by NMR, optical spectroscopy or electrochemical methods and purification by recrystallisation is foreclosed. On the other hand high yields were obtained. The main drawback however is that due to the insolubility of [(dppz)Pd(Me)Cl] the second reaction proceeds extremely slowly and filtration of precipitated AgCl leads to a huge loss of product decreasing the overall yields to 5–10%. Route B suffers mainly from the instability of the COD-complexes $[(COD)Pd(Me)L]^{n+}$. Both their formation and their reaction with RR′dppz ligands is accompanied by marked decomposition leading to black material (presumably elemental Pd). However, since the precursor complexes $[(COD)Pd(Me)L]^{n+}$ are readily available, all reactions occur rapidly and precursors and products are highly soluble, route B turned out to be more favourable. For the final products containing various N-donor ligands as cytosine (Cyt), 1-methylcytosine (1MeCyt), 1-methyluracilato (1MeUra), pyridine (Py) and caffeine (Caf, 1,3,7-trimethylxanthine) both routes were investigated, however only the variants with the best yield and purity were reported in the Experimental Section in detail.

While the neutral chlorido complexes were virtually insoluble, the cationic complexes $[(RR'dppz)Pd(Me)L]^{+}$ with $[SbF_6]^{-}$ counter ions exhibit fair to good solubility with a remarkably good solubility for the caffeine complexes. The neutral complex containing the 1-methyluracilato ligand [(dppz)Pd(Me)(1MeUra)] is almost insoluble. Due to these marked differences in solubility we have concentrated our efforts to generate a series using different RR′dppz ligands in complexes containing the caffeine co-ligand and another series using the parent dppz ligand and various co-ligands.

The obtained Pd-compounds were analysed by NMR spectroscopy. As expected, the two different co-ligands coordinating to the square planar configured Pd^{II} lower the symmetry of the symmetrical dppz ligands (C_{2v} to C_s) dppz and dcdppz. As a consequence all heteroaromatic protons exhibit individual signals. The unsymmetrical RR′dppz ligands show separate resonances

(^{1}H, ^{13}C) for the phenazine part, while for the bpy-part the signals for positions 1,8, 2,7 and 3,6 completely overlap.

For their complexes all heteroaromatic protons exhibit individual signals, however, no spectroscopic evidence was found for *E* or *Z* isomers in ^{1}H spectra. In the case of the caffeine complexes also the ^{13}C spectra (even at 600 MHz) did not show splitting of the signals, which would be expected for *E* and *Z* isomers. Since the discriminating effect should be most pronounced for complexes containing very different co-ligands we investigated the *in situ* generated solvent complex [(tfmdppz)Pd(Me)(Acetone)]$^+$. For this complex we were able to observe double sets of ^{13}C signals for the carbon atoms on the bpy part of the ligand with a splitting of the signals for the *E* and *Z* isomers of around 0.2 ppm (1 : 1 ratio), while no splitting for the corresponding ^{1}H signals could be observed (See ESI†). This is in line with previous findings on related complexes as [(CH_3dppz)Pd(Me)(MeCN)]$^+$.[5] Thus, an isomeric discrimination in the bpy-part of the dppz ligand is only possible for very different co-ligands (which is not the case for our complexes), while the phenazine is kind of "magnetically isolated" and does not show any sign of discrimination. This "isolation" is also evident from the fact that no ^{1}H ^{13}C or ^{13}C ^{13}C correlations are detectable across the connecting rings. This is also important for the further spectroscopic and electrochemical measurements where we also do not expect any discrimination of the *E* and *Z* isomers. The complete assignment of proton signals in Table 1 is based on ^{1}H COSY, ^{1}H NOESY for the complexes and additionally gradient selected ^{1}H, ^{13}C HSQC and HMBC experiments for the free ligands. The signal for the methyl co-ligand in the complexes is observed for all the Pd^{II} complexes around 1.0 ppm.

Crystal structure of [(dppz)Pd(Me)(Py)][SbF_6]

Single crystals of [(dppz)Pd(Me)(Py)][SbF_6] were obtained from a saturated toluene–acetone solution and the crystal and molecular structure were determined from XRD. The compound crystallised in the triclinic space group $P\bar{1}$ (for details see Table 2) and exhibits a number of intermolecular contacts, mainly due to π-stacking of the dppz ligand, while the pyridine co-ligand is not involved in such π-stacking (closest distance > 10 Å). The completely planar dppz ligands of complex molecules form two different types of layers (A and B), both with a tail-to-tail orientation (Fig. 1 and 2). The shortest distance between two molecules of

Table 1 Selected ^{1}H NMR data of the dppz ligands and palladium complexes[a]

Compounds	H1	H8	H3	H6	H10	H13	H2	H11	H12	H7	Solvent
adppz	9.59	9.59	9.23	9.23	7.37	8.14	7.76	—	7.37	7.76	$CDCl_3$
[(adppz)Pd(Me)(Caf)]$^+$	9.75	9.90	8.55	9.21	8.16	8.32	7.34	—	8.07	7.73	$(CD_3)_2CO$
dppz	9.67	9.67	9.29	9.29	8.37	8.37	7.81	7.94	7.94	7.81	$CDCl_3$
[(dppz)Pd(Me)Cl]	9.88	9.92	9.12	9.78	8.43	8.43	7.99	8.04	8.04	8.17	$CDCl_3$
[(dppz)Pd(Me)(1MeUra)]	9.69	9.80	8.69	9.13	8.40	8.40	7.90	8.02	8.02	8.17	$CDCl_3$
[(dppz)Pd(Me)(1MeCyt)]$^+$	9.70	9.77	8.77	9.18	8.35	8.35	8.19	8.19	8.19	8.35	$(CD_3)_2CO$
[(dppz)Pd(Me)(Cyt)]$^+$	9.87	9.99	8.84	9.25	8.49	8.49	8.25	8.20	8.20	8.38	$(CD_3)_2CO$
[(dppz)Pd(Me)(Caf)]$^+$	9.94	10.06	9.27	9.33	8.52	8.52	8.18	8.21	8.21	8.43	$(CD_3)_2CO$
cdppz	9.55	9.55	9.27	9.27	8.29	8.28	7.76	—	7.84	7.76	$CDCl_3$
[(cdppz)Pd(Me)Cl]	9.73	9.83	9.08	9.51	8.00	8.45	8.05	—	8.40	8.05	CD_2Cl_2
[(cdppz)Pd(Me)(Caf)]$^+$	9.80	9.94	8.45	9.33	8.67	8.45	8.15	—	8.45	8.15	$(CD_3)_2CO$
dcdppz	9.50	9.50	9.28	9.28	8.48	8.48	7.78	—	—	7.78	$CDCl_3$
[(dcdppz)Pd(Me)Cl]	9.72	9.82	9.54	9.10	8.60	8.60	8.06	—	—	8.06	CD_2Cl_2
[(dcdppz)Pd(Me)(Caf)]$^+$	9.83	9.98	8.69	9.33	8.70	8.70	8.17	—	—	8.42	$(CD_3)_2CO$
ndppz	9.63	9.63	9.33	9.33	9.27	8.50	7.84	—	8.67	7.84	$CDCl_3$
[(ndppz)Pd(Me)Cl]	9.86	9.95	9.25	9.50	9.33	8.77	8.40	—	8.89	8.40	DMF-D7
[(ndppz)Pd(Me)(Caf)]$^+$	9.94	10.09	8.72	9.38	9.31	8.76	8.22	—	8.87	8.47	$(CD_3)_2CO$
tfmdppz	9.39	9.39	9.22	9.22	8.52	8.32	7.70	—	8.00	7.70	$CDCl_3$
[(tfmdppz)Pd(Me)Cl]	9.77	9.88	9.11	9.54	8.19	8.78	8.07	—	8.60	8.07	CD_2Cl_2
[(tfmdppz)Pd(Me)(Caf)]$^+$	9.88	10.02	8.68	9.34	8.71	8.19	8.43	—	8.37	8.82	$(CD_3)_2CO$

[a] Chemical shifts/ppm; numbering of the protons according to Scheme 3; counter ion [SbF_6]$^-$.

Table 2 Crystal data of [(dppz)Pd(Me)(Py)][SbF_6][a]

Crystal system/space group	Triclinic/$P\bar{1}$	Indices	$-11 < h < 11$
Cell a/Å	9.1170(50)		$-12 < k < 12$
b/Å	10.1420(50)		$-21 < l < 21$
c/Å	16.5120(50)	$F(000)$/refl. coll.	695.9/21569
α (°)	82.022(5)	Data/restr./param.	6186/0/334
β (°)	80.729(5)	GOOF on F^2	1.096
γ (°)	68.043(5)	Final Rs [$I > 2\sigma(I)$]	0.0640/0.1658
V/Å^3; Z	1392.46(33); 2	Final Rs (all data)	0.1641/0.1660
Density/g cm^{-1}	1.71	R(int)	0.1293
μ/mm^{-1}	1.677	Largest peak diff.	3.111/−2.101

[a] Obtained by X-ray diffraction from single crystals at $T = 173(2)$ K, $\lambda = 0.71073$ Å, empirical formula: $C_{24}H_{18}N_5PdSbF_6$ (718.6 g mol^{-1}). Further details in the Experimental Section and the ESI.† The crystal structure contains disordered solvent molecules which could not be refined successfully, the corresponding electron density was squeezed. As a result the overall quality of the structure is poor.

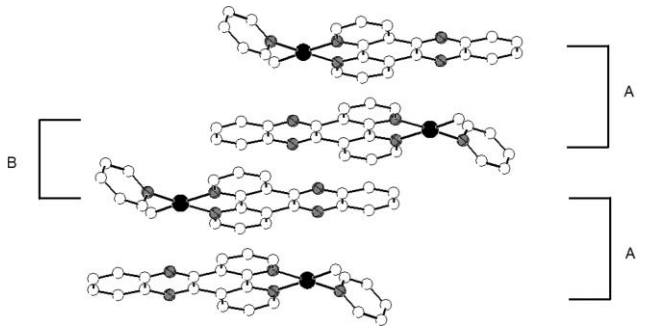

Fig. 1 Representation of the molecule layers with two different types of π-stacking in the crystal structure of [(dppz)Pd(Me)(Py)][SbF_6], protons and counter ions omitted for clarity.

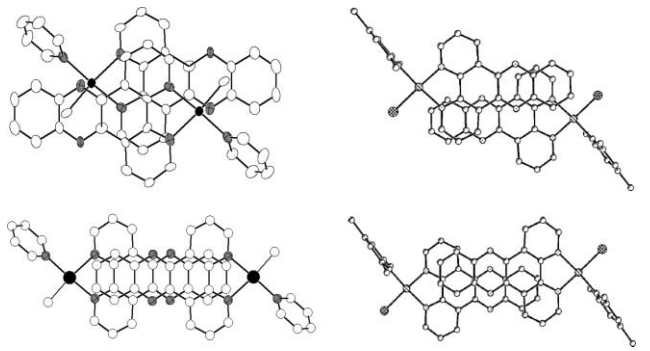

Fig. 2 Stacking in [(dppz)Pd(Me)(Py)][SbF_6] (left) and [(dppz)Ni(Mes)Br][12b] (right), each exhibiting two types of stacking in layer A (top) and layer B (bottom); The interlayer distances for [(dppz)Ni(Mes)Br] are 3.885(4) Å (layer A) and 3.796(5) Å (layer B); protons and counter ions are omitted for clarity.

such an A-layer is 3.362(7) Å, while the shortest distance for two molecules sharing a B-layer is 3.375(7) Å. Both values lie in the range of the stacking distance in graphite (3.8 Å). The previously reported complex [(dppz)Ni(Mes)Br][12b] which has a quite similar molecular structure also exhibits two types of dppz-stacked layers (Fig. 2) and it is interesting to note that altogether four different variations of dppz π-stacking are observed in these two structures, all with approximately the same stacking distance of 3.8 Å. Additionally to the π-stacking there are a number of H-bridging contacts in the crystal structure of [(dppz)Pd(Me)(Py)][SbF_6], mainly between dppz protons and the fluorine atoms of the counter ions (the shortest contacts are listed in the ESI†). However, all of these contacts are quite long (shortest: 2.420(5) Å) and we do not suppose that they have a marked influence on the complex molecule geometry.

While the dppz ligand is completely coplanar to the coordination plane (*N*,*N*,Pd,C,N) the molecular structure of [(dppz)Pd(Me)(Py)]$^+$ reveals that the pyridine co-ligand is markedly tilted with a torsion angle of 63.448(4)°, which circumvents intermolecular stacking in this part of the molecule (see above). The ligand bite angles around the Pd atom sum up to 360° [with N_{dppz}–Pd–N_{dppz} = 79.731(17)°; N_{dppz}–Pd–N_{py} = 97.491(18)°; N_{dppz}–Pd–C = 94.571(19)°; N_{py}–Pd–C = 88.318(17)°]. The distance Pd–N_{py} = 2.0390(5) Å is comparable to the *trans* located N_{dppz}–Pd = 2.0243(5) Å bond length, while the *cis* located N_{dppz}–Pd = 2.1404(9) Å is markedly longer. This is in line with the expected *trans* influence of the strong methyl co-ligand (C–Pd = 2.0382(8) Å).

Absorption and emission spectra

All free ligands and the corresponding Pd^{II} complexes [(RR′dppz)Pd(Me)(Caf)][SbF_6] (Caf = caffeine) were submitted to a comparative study of their absorption and luminescence properties. Generally, dppz complexes have been intensely investigated for their interesting photophysical properties to which they owe their special orbital occupation (see Introduction).[17,32] The ligands all show strong (and partly structured) absorption bands in the range of 200–300 nm (λ_{Abs1} in Table 3) which can be assigned to π–π* transition in the bipyridine part of the dppz ligand[10c] and bands in the range of 350–400 nm (λ_{Abs2} and λ_{Abs3} in Table 3), which are due to π–π* transition centred in the phenazine part of the ligand.[10b,32]

In comparison to many other dppz complexes of low-valent metals as Ru^{II} or Pt^{II} [8,13] no metal-to-ligand charge transfer (MLCT) absorption bands were observed in the visible range. We suppose that they occur at wavelengths < 380 nm and were thus obscured by the strong intra-ligand transitions. Our assumption is based on comparison to related Ni^{II} and Pt^{II} complexes *e.g.* the complex [(dppz)Ni(Mes)Br] exhibits a long-wavelength

Table 3 Main absorption and emission maxima of selected RR′dppz ligands and complexes[a]

Compound	λ_{Abs1}	λ_{Abs2}	λ_{Abs3}	λ_{Exc}[b]	λ_{Em}[c]	ϕ 10^{-3}[d]
Tfmdppz	293 (27)	360 (14)	379 (14)	410	521	4.99
[(tfmdppz)Pd(Me)(Caf)]$^+$	272 (87)	360 (15)	378 (15)	470	585	2.13
dppz	293 (34)	359 (20)	379 (21)	400	535	12.3
[(dppz)Pd(Me)(Caf)]$^+$	292 (30)	360 (18)	379 (20)	450	565	6.20
cdppz	292 (21)	366 (14)	386 (17)	420	515	0.66
[(cdppz)Pd(Me)(Caf)]$^+$	275 (51)	369 (11)	389 (12)	450	625	24.7
ndppz	298 (42)	373 (16)	391 (14)	410	513	46.7
[(ndppz)Pd(Me)(Caf)]$^+$	286 (55)	371 (14)	391 (11)	450	575	60.9
dcdppz	295 (24)	371 (18)	392 (26)	500	543	1.63
[(dcdppz)Pd(Me)(Caf)]$^+$	278 (81)	372 (17)	393 (22)	460	578	9.42
adppz	293 (69)[e]	308 (70)[e]	447 (26)[e]	470	558	1.07
[(adppz)Pd(Me)(Caf)]$^+$	304 (205)	391(49)	472 (53)	450	586	17.99

[a] Measured in DMF, absorption, excitation and emission maxima λ/nm, for absorption maxima with molar extinction coefficients $\varepsilon/10^3$ dm^3 mol^{-1} cm^{-1} in parentheses. [b] Excitation maxima obtained from excitation spectra recorded on the maximum value for the long-wavelength emission. [c] Emission maxima recorded upon irradiation at λ_{Exc}. [d] Quantum yield. [e] From ref. 28.

absorption band at 467 nm,[12b] [(dppz)Pt(Mes)Cl] at 428 nm, while for [(dppz)Pd(Mes)Cl] the band is shifted to $\lambda < 380$ nm (all in DMF). The thus observed sequence $Pd^{II} > Pt^{II} > Ni^{II}$ for the long-wavelength MLCT energy is in agreement with decreasing 2nd ionisation energies (IE): 19.43 eV for Pd > 18.56 eV for Pt > 18.17 eV for Ni[33] and also with increasing valence p-electron binding energies: 50.9 eV (Pd-4p) < 51.7 eV (Pt-5p) < 66.2 eV (Ni-3p).[34] Instead of being directly visible through detectable MLCT transitions the coordination of Pd^{II} to the RR′dppz ligand has a marked effect on the intensities of the intra-ligand absorption bands. While the extinction coefficients ε decrease for the phenazine-centred transitions, absorptions in the bipyridine part gain in intensity. The energy of the long-wavelength absorption bands of the substituted dppz ligands follow the series dppz ≅ tfm > cdppz > dcdppz ≅ ndppz > adppz. The adppz ligand exhibits the lowest energy absorption which is due to the stabilisation of the lowest two singlet excited states.[35] In this context it is difficult to rationalise why electron-withdrawing groups NO_2 and Cl also exhibit a bathochromic shift compared to dppz as observed for the electron-releasing NH_2 group. Furthermore, substitution with CF_3 has almost no effect. The corresponding complexes $[(RR'dppz)Pd(Me)(Caf)]^+$ interestingly do not follow the above series of bathochromic shift, although the transitions should still be the same after coordination (phz-based).

All free ligands and their Pd^{II} complexes exhibit luminescence at ambient temperature in DMF solution. When irradiating into the long-wavelength absorption band, emission maxima ranging from 450 (dppz) to 625 nm (dcdppz) were detected with quantum yields varying from 0.06 to 0.0007. In most cases the complexes exhibit lower emission energies and at the same time higher quantum yields in comparison to the free ligands (the latter is not true for tfmdppz and dppz). This is contrary to the energy-gap-law[36] and points to a complex emission behaviour. Also, the emission energies do not correlate to the maximum absorption energy (λ_{Abs3}), or in other words the Stokes-shifts vary largely from 1600 to 6200 cm^{-1} (see ESI†). Obviously the origin of the emission is not the same for all ligands and complexes. This is not unexpected in view of the complex luminescence behaviour of the free ligand dppz.[17] Since the substitution and coordination gives rise to a marked altering of the luminescence it would be worth studying the luminescence properties of our complexes in detail, including the investigation of life-times. Such a study is under way.

Electrochemical properties and EPR spectroscopy

The redox properties of the dppz derivatives and of selected Pd^{II} complexes were studied in DMF solutions. All systems exhibit a number of reduction waves (at least three), while only the Pd^{II} complexes can be oxidised in the accessible potential range. While many of the one-electron reduction processes occur reversibly, the one-electron oxidations (all around 0.3 V) are irreversible. Fig. 3 shows two representative examples, Table 4 lists data of the free ligands and selected complexes (Cl or caffeine co-ligands), complete data is supplied in the ESI.†

The first reduction potential for the free ligands decreases along the series ndppz > tfmdppz > dcdppz > cdppz > dppz > adppz. In contrast to the long-wavelength absorptions this series reflects the expected electron-withdrawing (NO_2, CF_3, Cl) or electron-releasing (NH_2) effects of the substituents. For the corresponding complexes these series can also be observed, while the absolute values were increased by only about 0.1 to 0.2 V and the differences between corresponding positively charged and neutral complexes is even smaller (0.05 to 0.1 V). The latter difference is virtually zero for ndppz complexes. Calculating the differences between the first and second reduction potential ($\Delta E_{Red1} - E_{Red2}$) (Table 4) reveals that the differences for all ligands and complexes are about 0.8 V with the exception of ndppz and its complexes ($\Delta E_{Red1} - E_{Red2} \sim 0.5$ V). In similarity to a number of investigated dppz complexes of various transition metals we can assign the first reduction potential of all ligands and complexes to the phenazine-based b_1 π* orbital as the lowest unoccupied MO. The large values of about 0.8 for $\Delta E_{Red1} - E_{Red2}$ indicate that the second reduction is also phenazine-based. Related values have been observed for dppz complexes of Pt^{II}, Mo^0, Cu^I and Re^I.[2,8]

An interesting aspect is that the chlorido complexes [(RR′dppz)Pd(Me)Cl] exhibit an irreversible second reduction, while these waves are reversible for the cationic counterparts. We assume that the irreversibility is caused by the splitting of the chlorido ligand after the second reduction. This behaviour has been investigated in detail for corresponding nickel complexes [(N∧N)Ni^{II}(Mes)X] (N∧N = various α-diimine chelate ligands

Table 4 Electrochemical data of RR′dppz ligands and selected complexes[a]

Compound	$E_{1/2}$ Red 1	$E_{1/2}$ Red 2 or E_{pc}	$\Delta E_{Red1} - E_{Red2}$
ndppz	−1.19	−1.74	0.55
tfmdppz	−1.38	−2.14	0.80
dcdppz	−1.42	−2.14	0.78
cdppz	−1.53	−2.31	0.80
dppz	−1.64	−2.26	0.78
adppz	−1.85	−2.57	0.72
$[(ndppz)Pd(Me)(Caf)]^+$	−1.03	−1.56	0.57
$[(tfmdppz)Pd(Me)(Caf)]^+$	−1.20	−2.02	0.72
$[(dcdppz)Pd(Me)(Caf)]^+$	−1.23	−2.06	0.79
$[(cdppz)Pd(Me)(Caf)]^+$	−1.27	−2.01	0.73
$[(adppz)Pd(Me)(Caf)]^+$	−1.38	−2.14	0.78
$[(dppz)Pd(Me)(Caf)]^+$	−1.44	−2.21	0.86
[(ndppz)Pd(Me)Cl]	−1.04	−1.55	0.51
[(tfmdppz)Pd(Me)Cl]	−1.25	−1.96 (irr)	0.74[b]
[(dcdppz)Pd(Me)Cl]	−1.33	−2.03 (irr)	0.74[b]
[(cdppz)Pd(Me)Cl]	−1.34	−1.93 (irr)	0.69[b]
[(dppz)Pd(Me)Cl]	−1.35	−2.06 (irr)	0.71[b]

[a] Potentials in V *vs.* ferrocene/ferrocenium from cyclic voltammetry or square wave voltammetry in 0.1 M DMF/$n$$Bu_4NPF_6$ solutions at 298 K; Half wave potentials $E_{1/2}$ given for reversible processes, E_{pc} for irreversible processes. B for the calculation of $\Delta E_{Red1} - E_{Red2}$ $E_{pc(Red2)}$ was used for rendering these values less accurate.

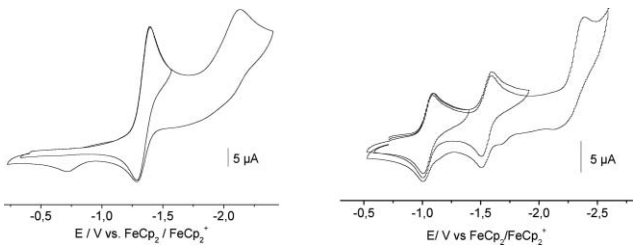

Fig. 3 Cyclic voltammograms of [(dppz)Pd(Me)Cl] in $n$$Bu_4NPF_6$/DMF solution (left) and [(ndppz)Pd(Me)Cl] $n$$Bu_4NPF_6$/DMF solution (right) at ambient temperature and 100 mV s^{-1} scan rate.

such as bpy or phen; Mes = mesitylene; X = halogenido).[37] Although, for the nickel complexes reduction occurs essentially diimine-ligand based, the X-co-ligand is rapidly cleaved after one-electron uptake. Since dppz, compared to the α-diimine ligands used in this study, is superior concerning the stabilisation of extra electrons, the first reduction of the complexes [(RR′dppz)Pd(Me)Cl] occurs reversibly, and only the second leads to the cleavage of Cl^-. The cationic complexes $[(RR'dppz)Pd(Me)(Caf)]^+$ do obviously not cleave their caffeine co-ligand, which is either due to the charge or the π-acceptor character of all of this ligand. For the corresponding ndppz complex [(ndppz)Pd(Me)Cl] the second reduction is also completely reversible (Fig. 3). Furthermore, as mentioned already above for the ndppz ligand and its complexes $\Delta E_{Red1} - E_{Red2}$ values of about 0.5 V were observed. Very obviously, in these cases the reduction behaviour is markedly altered through the substituent -NO_2.

To verify this hypothesis EPR experiments and DFT calculations were carried out on the mono-reduced states of the ligands ndppz and adppz (the latter representing the majority of the RR′dppz ligands) and their Pd^{II} complexes $[(RR'dppz)Pd(Me)(Caf)][SbF_6]$ at ambient temperature. Upon *in situ* reduction of the adppz ligand a five-line signal is observed at $g = 2.0038$ (Fig. 4). Such hyperfine splitting has been observed for dppz and also many dppz complexes and is due to the dominant coupling of the unpaired electron to the two nitrogen atoms (^{14}N, $I = 1$, 99.636% nat. abundance) in the phenazine ring. The spectral simulation was carried out assuming two coupling constants a_N of 0.596 and 0.437 mT respectively for the two (magnetically non-equivalent) phenazine N atoms, the corresponding value for dppz is 0.505 mT.[8] While Kaim *et al.* also reported coupling constants $a_{N4,5}$ of 0.021 mT and $a_{H10,13}$ of 0.183 mT[8] we were not able to include further nuclei into our simulation due to the poor spectral resolution. Nevertheless, we can state that the amino group does not contribute markedly to the singly occupied molecular orbital (SOMO), while the asymmetric substitution leads to slight asymmetry between the contributions of N9 and N14. For ndppz a far more complicated signal was obtained (Fig. 4, $g = 2.0053$), for which the simulation yielded coupling constants $a_N(phz) = 0.350$ and 0.317 mT and $a_N(NO_2) = 0.234$ mT respectively. Further splitting was simulated assuming contributions from H10 (0.084 mT, H13 (0.067 mT) and H12 (0.055 mT). The electron density of the SOMO was calculated by DFT for adppz and ndppz confirming that for the NO_2-derivative marked spin-density is located in the substituent, while the NH_2-group does not participate (Fig. 4; for details of the calculations see ESI†).

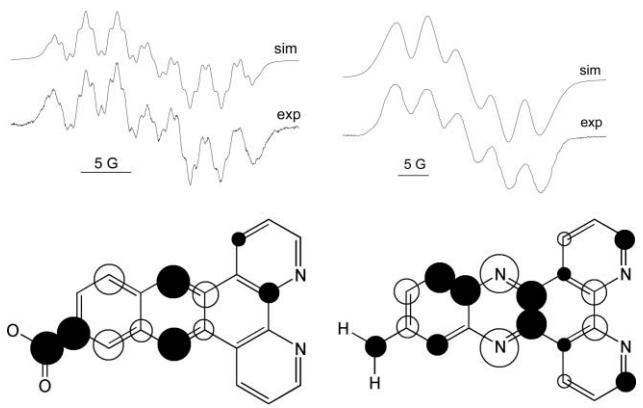

Fig. 4 Top: a) EPR spectra and simulation of electrochemically reduced ndppz (left) and adppz (right), both generated and measured in CH_2Cl_2/nBuNPF$_6$ at 298 K. Bottom: Calculated (B3-LYP, TZVP) electron density for the LUMOs of ndppz (left) and adppz (right).

The Pd complexes $[(ndppz)Pd(Me)(Caf)][SbF_6]$ and $[(adppz)Pd(Me)(Caf)][SbF_6]$ were electrolysed in a THF–DMF mixture and spectra were recorded at 298 K. In both cases unresolved broad isotropic lines were observed with $g = 2.0055$ for the ndppz complex (total spectral width $\Delta H = 28$ mT) and 2.0037 for the adppz derivative ($\Delta H = 48$ mT). Their *g*-values match closely with those of the corresponding uncoordinated dppz-ligands.

Cytotoxicity

Finally, selected complexes were evaluated for their effects on cell growth inhibition of HT-29 colon carcinoma and MCF-7 breast adenocarcinoma cells (see Table 5). Since dppz was recently tested for its antiproliferative effects,[38] two corresponding organometallic Pd complexes were chosen, one containing a biorelevant co-ligand (1MeUra). Furthermore, Pd complexes of two substituted dppz-derivatives (dcdppz and tfmdppz) were tested in comparison to the free ligands. This choice was motivated from the question if the substitution inhibits DNA intercalation and thus markedly decreases the antiproliferative effect. Interestingly, for some of the complexes promising antiproliferative effects in the range of the well known anticancer drug cisplatin could be noted. The complexes [(dppz)Pd(Me)(1MeUra)], [(dcdppz)Pd(Me)Cl] and $[(tfmdppz)Pd(Me)(Caf)][SbF_6]$ were the most active compounds in this series, whereas [(dppz)Pd(Me)Cl] and [(tfmdppz)Pd(Me)Cl] were either inactive or of lower activity. The free ligands dcdppz and tfmdppz were used as references and afforded cell growth inhibitory activity for tfmdppz but not for dcdppz. For the dcdppz derivative this indicates that complexation led to a substantial increase in biological activity. For the tfmdppz derivatives activity could be increased upon complexation for $[(tfmdppz)Pd(Me)(Caf)][SbF_6]$ but not for its neutral methyl chlorido analogue [(tfmdppz)Pd(Me)Cl]. As we noted for the dppz ligand IC_{50} values below 2 μM in a previous study[39] it can be concluded that in the case of [(dppz)Pd(Me)Cl] and [(dppz)Pd(Me)(1MeUra)] complexation had a negative effect on the triggering of antiproliferative effects. The related Pt^{II} complex $[Pt(dppz)(t\text{N}\wedge\text{C})]CF_3SO_3$ (tN∧C = 4-*tert*-butyl-2-phenylpyridine) has been reported to exhibit high antiproliferative effects when tested against KB-3-1 and KB-V1 cell lines with

Table 5 Cytotoxicity of selected compounds in HT-29 and MCF-7 cells expressed as IC_{50} values obtained in two independent experiments

Compound	IC_{50} HT-29/μM[a]	IC_{50} MCF-7/μM[b]
cisplatin[c]	7.0 ±2.0	2.0 ±0.3
[(dppz)Pd(Me)Cl]	> 100	> 100
[(dppz)Pd(Me)(1MeUra)]	3.7 ± 1.3	1.9 ± 0.2
[(dcdppz)Pd(Me)Cl]	2.2 ± 0.4	2.8 ± 1.6
dcdppz	> 100	> 100
[(tfmdppz)Pd(Me)Cl]	> 100	9.8 ± 10.5
$[(tfmdppz)Pd(Me)(Caf)][SbF_6]$	5.1 ± 0.1	1.6 ± 0.1
tfmdppz	10.2± 4.8	7.2± 2.7

[a] Incubation time 72 h. [b] Incubation time 96 h. [c] From ref. 38

LD_{50} values of 1.7 ± 0.5 and 1.0 ± 0.5 μMol compared to cisplatin (22.1 ± 3.6 and 39.1 ± 1.7 respectively). Unfortunately, from this small number of examples we cannot draw unequivocal structure–activity correlations and further testing is necessary. In general, the cytotoxic effects of polypyridyl complexes seem to be the consequence of multiple factors including the size of the polypyridyl ligands and cellular uptake.[38-42] Distinctive effects on cellular metabolism[39,42] and cell membrane integrity[42,43] have been reported recently highlighting the complicated biological profile of these species and suggesting a more detailed biological evaluation of these type of metal complexes.

However, one important thing can be concluded from our experiment, that is that the complexes remain stable under the experimental conditions and do not produce free dppz ligand.

Conclusions

For the synthesis of the new organometallic palladium complexes of the type $[(RR'dppz)Pd(Me)L]^{n+}$ (RR′dppz = derivatives of dipyrido[3,2-*a*:2′,3′-*c*]phenazine with RR′ = 11-Cl, 11,12-Cl_2, 11-CF_3, 11-NO_2, 11-NH_2; L = Cl, 1-methyluracilate (n = 0), pyridine, cytosine, caffeine, or 1-methylcytosine, (all n = 1) two alternative routes were described. However due to the extremely bad solubility of the neutral complexes [(RR′dppz)Pd(Me)Cl] the route *via* the COD derivatives $[(COD)Pd(Me)L]^{n+}$ gave higher yields in shorter time and is more promising for further related synthesis. UV/Vis absorption and emission data gives no clear correlation for influence of the electron-withdrawing or -releasing substituents which is due to the very complex excited state properties of dppz and its derivatives. Complexation with Pd^{II} does not alter this complicated behaviour. In contrast to this, electrochemical investigations reveal that CF_3 and Cl exert a general electron-withdrawing effect, while NH_2 releases electron-density, as expected. The electrochemical and EPR results point to mainly phenazine-centred first and second reductions. A closer inspection of adppz and ndppz and their complexes by EPR spectroelectrochemistry combined with quantum chemical calculations (DFT) reveals the expected asymmetric distribution of the electron density of the phenazine-based LUMO. The most interesting substituent is 11-NO_2, which markedly alters the LUMO/SOMO exhibiting high spin-density of the SOMO on the NO_2 nitrogen atom and a reductive electrochemistry at rather high potentials. Generally, the Pd complex fragments $[Pd(Me)L]^{n+}$ (n = 0 or 1) form stable bonds to the dppz ligands but their electronic influence is far smaller than observed *e.g.* for Ru^{II}, Pt^{II} or Cu^{I} complex fragments. This is obvious from very high energy MLCT transitions and very small stabilisation of the LUMOs (by 0.1 to 0.2 V) upon coordination. Nevertheless, the complexes seem to remain stable during cytotoxicity experiments on HT-29 colon carcinoma and MCF-7 breast cancer cell lines. And the results of this preliminary study revealed promising activities for some of the compounds.

Experimental

Instrumentation

Elemental analyses were carried out on HEKAtech CHNS EuroEA 3000 Analyzer. NMR spectra were recorded on Bruker Avance II 300 MHz (^{1}H: 300.13 MHz, ^{13}C: 75.47 MHz, ^{19}F: 282.35 MHz), Bruker Avance 400 MHz (^{1}H: 400.13 MHz, ^{13}C: 100.61 MHz, ^{19}F: 376.50 MHz), using a triple resonance ^{1}H,^{19}F,BB inverse probe head or a Bruker Avance II 600 MHz (^{1}H: 600.23 MHz, ^{13}C: 150.93 MHz). The unambiguous assignment of the ^{1}H and ^{13}C resonances was obtained from ^{1}H COSY, ^{1}H NOESY, gradient selected ^{1}H, ^{13}C HSQC and HMBC experiments. All ^{2}D-NMR experiments were performed using standard pulse sequences from the Bruker pulse program library. Chemical shifts were relative to TMS for ^{1}H and ^{13}C, and CCl_3F for ^{19}F. Due to the fact that the signals of the aromatic ligands in the ^{1}H spectra are of higher order, the assignments (d or dd *etc.*) of the multiplicity of the signals denote only the observed shape of the signals. Thus coupling constants were not given. UV/Vis absorption spectra were measured using a Varian Cary50 Scan photospectrometer. UV/Vis emission spectra were obtained using a Spex FlouroMax-3 spectrometer. Electrochemical studies were carried out on an Autolab PGSTAT30 potentiostat and function generator in 0.1 M nBu$_4$NPF$_6$/DMF solutions using a three-electrode configuration (glassy carbon working electrode, Pt counter electrode, Ag/AgCl reference). Half-wave ($E_{1/2}$), anionic (E_{pa}) or cationic peak potentials (E_{pc}) are given with respect to the ferrocene/ferrocenium couple, which also serves as internal reference. EPR spectra were recorded in the X band using a Bruker ELEXSYS 500E equipped with a Bruker Variable Temperature Unit ER 4131VT.

Crystal structure determination

Performed at 173(2) K, using graphite-monochromatised Mo-Kα radiation (λ = 0.71073 Å) on an IPDS I (STOE and Cie). The crystal was fixed in a loop with frozen fluorinated oil. The structure was solved by direct methods (SHELXS-97)[44] and refined by full-matrix least-squares techniques against F^2 (SHELXL-97).[45] Absorption correction was carried out using X-RED and X-SHAPE (STOE).[46] The non-hydrogen atoms were refined with anisotropic displacement parameters without any constraints. The hydrogen atoms were included by using appropriate riding models.

Quantum chemical calculations

DFT calculations with B3-LYP[47] function and basis set TZVP[48,49a] were performed with the program *Turbomol*[49] using a z-matrix produced with *GaussView*[50] using standard bond-lengths and -angles, and idealising the dppz scaffold to be completely planar. Doing so, one ignores a ring-torsion vibration, occurring for the ring connecting the bipyridine part and the phenazine part. This simplification is justified as dppz is known to be completely planar in crystal structures. Results were visualised with the program *Molden*.[51]

Cytotoxicity

The antiproliferative effects of the compounds were determined following an established procedure.[38] In short, cells were suspended in cell culture medium (HT-29: 2850 cells mL^{-1}, MCF-7: 10000 cells mL^{-1}), and 100 μL aliquots thereof were plated in 96 well plates and incubated at 37 °C: 5% CO_2 for 48 h (HT-29) or 72 h (MCF-7). The compounds were freshly diluted/suspended in dimethylformamide (DMF) and the resulting

solutions/suspensions were diluted with cell culture medium to the desired concentrations (final DMF concentration: 0.1% v/v). The medium in the plates was replaced with medium containing the compounds in graded concentrations (six replicates). After further incubation for 72 h (HT-29) or 96 h (MCF-7) the cell biomass was determined by crystal violet staining and the IC_{50} values were determined as those concentrations causing 50% inhibition of cell proliferation. Results were calculated from two independent experiments.

Materials and procedures

Solvents (CH_2Cl_2, THF, toluene, diethyl ether and MeCN) were dried using a MBRAUN MB SPS-800 solvent purification system. All preparations and physical measurements in this work were carried out in dry solvents under argon, using Schlenk techniques. 1,10-phenanthroline was supplied from Chempur, $AgSbF_6$ from ABCR. Cytosine and Pd/C (10%) were obtained from Fluka, caffeine was obtained from Acros Organics and *o*-phenylenediamines were obtained from Alfa Aesar. 1,10-Phenanthrolinedione (pdo)[52] and dppz[7n] and the derivatives ndppz,[24,28] adppz[28] and cdppz[5,24] were synthesised according to literature procedures. 1-Methylcytosine was prepared following a procedure published by Kistenmacher *et al.*[53] The palladium precursor complexes [(COD)Pd(Me)Cl][30] and [(COD)Pd(Me)L][SbF_6] (L = cytosine, 1-methylcytosine, 1-methyluracil and caffeine)[31] were synthesised as previously described.

General procedure for the Schiff base condensation of dppz-derivatives

In a typical reaction 1 eq (14 mmol, 3.0 g) of pdo was mixed with 300 mL ethanol to give an incomplete solution. The corresponding *o*-phenylenediamine (14 mmol, 1 eq) was dissolved in ethanol and both mixtures were combined and stirred at 80 °C overnight. The solvent was removed under vacuum to yield the products as solids. The crude products were recrystallised from methanol.

tfmdppz. Yield: 78% of a colourless solid. (Found: C, 65.25; H, 2.34; N, 15.25. Calc. for $C_{19}H_9F_3N_4$: C, 65.15; H, 2.59; N, 15.39%); δ_H(300 MHz; $CDCl_3$): 9.39 (2 H, m, $H_{1,8}$), 9.22 (2 H, m, $H_{3,6}$), 8.52 (1 H, s, H_{10}), 8.32 (1 H, dd, H_{13}), 8.00 (1 H, dd, H_{12}), 7.70 (2 H, m, $H_{2,7}$); δ_F(376.50 MHz; $CDCl_3$):–62.62 (3 F, s, CF_3).

dcdppz. Yield: 77% of a grey powder. (Found: C, 61.44; H, 2.24; N, 15.82. Calc. for $C_{18}H_8Cl_2N_4$: C, 61.56; H, 2.30; N, 15.95%); δ_H(300 MHz; $CDCl_3$): 9.50 (2 H, m, $H_{1,8}$), 9.28 (2 H, m, $H_{3,6}$), 8.43 (2 H, d, $H_{10,13}$), 7.78 (2 H, d, $H_{2,7}$).

General procedure for the synthesis of [(RR′dppz)Pd(Me)Cl]

The precursor complex [(COD)Pd(Me)Cl] (1 eq) was dissolved in CH_2Cl_2. Then a solution of the desired RR′dppz ligand (1 eq) in toluene was added to the reaction mixture. The reaction was performed at ambient temperature overnight. The formed solid was filtered off and washed with acetone : pentane, 1 : 1 to yield the pure products.

[(dppz)Pd(Me)Cl]. Yield: 88% of a yellow solid. (Found: C, 51.99; H, 2.91; N, 12.76. Calc. For $C_{19}H_{13}Cl_1N_4Pd$: C, 51.96; H, 2.98; N, 12.76%); δ_H(300 MHz; $CDCl_3$): 9.92 (1 H, dd, H_{dppz8}), 9.88 (1 H, dd, H_{dppz6}), 9.78 (1 H, dd, H_{dppz1}), 9.64 (1 H, dd, H_{dppz3}), 8.43 (2 H, m, $H_{dppz10,13}$), 8.17 (1 H, dd, H_{dppz7}), 8.04 (2 H, dd, $H_{dppz11,12}$), 7.99 (1 H, dd, H_{dppz2}), 1.17 (3 H, s, $H_{Pd\text{-}CH3}$).

[(tfmdppz)Pd(Me)Cl]. Yield: 66% of a colourless solid. (Found: C, 47.32; H, 2.41; N, 11.01. Calc. for $C_{20}H_{12}Cl_1F_3N_4Pd$: C, 47.36; H, 2.38; N, 11.05%); δ_H(300 MHz; CD_2Cl_2): 9.88 (1 H, m, H_{dppz8}), 9.77 (1 H, m, H_{dppz1}), 9.54 (1 H, dt, H_{dppz6}), 9.11 (1 H, dt, H_{dppz3}), 8.78 (1 H, s, H_{dppz10}), 8.60 (1 H, dd, H_{dppz13}), 8.19 (1 H, dd, H_{dppz12}), 8.07 (2 H, m, $H_{dppz2,7}$), 1.14 (3 H, s, $H_{Pd\text{-}CH3}$).

[(cdppz)Pd(Me)Cl]. Yield: 82% of a grey solid. (Found: C, 48.22; H, 2.53; N, 11.87. Calc. For $C_{19}H_{12}Cl_2N_4Pd$: C, 48.18; H, 2.55; N, 11.83%); δ_H(300 MHz; CD_2Cl_2): 9.83 (1 H, dd, H_{dppz8}), 9.73 (1 H, dd, H_{dppz1}), 9.51 (1 H, dd, H_{dppz6}), 9.08 (1 H, dd, H_{dppz3}), 8.45 (1 H, d, H_{dppz10}), 8.40 (1 H, d, H_{dppz13}), 8.05 (2 H, m, $H_{dppz2,7}$), 8.00 (1 H, m, H_{dppz12}), 1.13 (3 H, s, $H_{Pd\text{-}CH3}$).

[(ndppz)Pd(Me)Cl]. Yield: 99% of an orange solid. (Found: C, 47.12; H, 2.52; N, 14.49. Calc. for $C_{19}H_{12}Cl_1N_5O_2Pd$: C, 47.13; H, 2.50; N, 14.46%); δ_H(300 MHz; $(CD_3)_2NCO$): 9.95 (1 H, m, H_{dppz8}), 9.86 (1 H, m, H_{dppz1}), 9.50 (1 H, m, H_{dppz6}), 9.33 (1 H, s, H_{dppz10}), 9.25 (1 H, m, H_{dppz12}), 8.89 (1 H, m, H_{dppz13}), 8.77 (1 H, m, H_{dppz3}), 8.40 (1 H, m, H_{dppz7}), 1.19 (3 H, s, $H_{Pd\text{–}CH3}$).

[(dcdppz)Pd(Me)Cl]. Yield: 84% of a greenish solid. Found: C, 48.30; H, 2.36; N, 11.82. Calc. for $C_{19}H_{11}Cl_2N_4Pd$: C, 48.29; H, 2.35; N, 11.85%); δ_H(300 MHz; CD_2Cl_2): 9.82 (1 H, dd, H_{dppz8}), 9.72 (1 H, dd, H_{dppz1}), 9.54 (1 H, dd, H_{dppz6}), 9.10 (1 H, dd, H_{dppz3}), 8.60 (2 H, d, $H_{dppz10,13}$), 8.06 (2 H, m, $H_{dppz2,7}$), 1.14 (3 H, s, $H_{Pd\text{-}CH3}$).

General procedure for the preparation of complexes [(RR′dppz)Pd(Me)(L)][SbF_6] from [(COD)Pd(Me)(L)]$^{n+}$ (Route B)

An appropriate amount of [(COD)Pd(Me)(L)]$^{n+}$ (0.95 eq) dissolved in 50 mL of THF was admixed to a solution of the RR′dppz ligand in 50 mL of toluene and 1–2 mL of methanol and the mixture was stirred at ambient temperature overnight. Solvents were removed under vacuum at ambient temperature to yield the crude products as coloured solids. The solids were washed with acetone to remove free COD and RR′dppz and yield pure products.

[(dppz)Pd(Me)(1MeCyt)][SbF_6]. Yield: 75% of a yellow solid. (Found: C, 37.73; H, 2.70; N, 12.84. Calc. for $C_{24}H_{20}F_6N_7OPdSb$: C, 37.70; H, 2.64; N, 12.82%); δ_H(300 MHz; $(CD_3)_2CO$): 9.77 (1 H, dd, H_{dppz8}), 9.70 (1 H, dd, H_{dppz1}), 9.18 (1 H, dd, H_{dppz6}), 8.77 (1 H, dd, H_{dppz3}), 8.35 (3 H, m, $H_{dppz7,10,13}$), 8.19 (3 H, m, $H_{dppz2,11,12}$), 7.99 (1 H, d, H_{1MeCy6}), 6.22 (1 H, d, H_{1MeCy5}), 3.60 (3 H, s, $H_{1MeCy\text{-}CH3}$), 0.98 (3 H, s, $H_{Pd\text{–}CH3}$).

[(dppz)Pd(Me)(1MeUra)]. Yield: 16% of a pale red solid. (Found: C, 54.51; H, 3.40; N, 15.89. Calc. for $C_{24}H_{18}N_6O_2Pd$: C, 54.51; H, 3.43; N, 15.89%); δ_H(300 MHz; $CDCl_3$): 9.80 (1 H, m, H_{dppz8}), 9.83 (1 H, m, H_{dppz1}), 9.13 (1 H, m, H_{dppz6}), 8.69 (1 H, m, H_{dppz3}), 8.40 (2 H, m, $H_{dppz12,13}$), 8.17 (1 H, m, H_{dppz7}), 8.02 (2 H, m, $H_{dppz11,12}$), 7.90 (1 H, m, H_{dppz2}), 7.15 (1 H, d, H_{1MeU6}), 5.80 (1 H, d, H_{1MeU5}), 3.45 (3 H, s, $H_{1MeU\text{-}CH3}$19), 1.08 (3 H, s, $H_{Pd\text{–}CH3}$).

[(dppz)Pd(Me)(Cyt)][SbF_6]. Yield: 68% of a yellow solid. (Found: C, 36.87; H, 2.46; N, 13.05. Calc. for $C_{23}H_{18}F_6N_7OPdSb$: C, 36.80; H, 2.42; N, 13.06%); δ_H(300 MHz; $(CD_3)_2CO$): 9.99 (1 H, dd, H_{dppz8}), 9.87 (1 H, dd, H_{dppz1}), 9.25 (1 H, dd, H_{dppz6}), 8.84 (1 H,

dd, H_{dppz3}), 8.49 (2 H, m, $H_{dppz10,13}$), 8.38 (1 H, m, H_{dppz7}), 8.25 (1 H, m, H_{dppz2}), 8.20 (2 H, m, $H_{dppz11,12}$), 7.90 (1 H, d, H_{Cyt6}), 6.22 (1 H, d, H_{Cyt5}), 1.00 (3 H, s, H_{Pd-CH3}).

[(dppz)Pd(Me)(Caf)][SbF$_6$]. Yield: 42% of a colourless solid. (Found: C, 38.97; H, 2.77; N, 13.41. Calc. for $C_{27}H_{23}F_6N_8O_2PdSb$: C, 38.90; H, 2.78; N, 13.44%); δ_H(300 MHz; $(CD_3)_2CO$): 10.06 (1 H, m, H_{dppz8}), 9.94 (1 H, m, H_{dppz1}), 9.33 (1 H, m, H_{dppz6}), 9.27 (1 H, s, H_{dppz3}), 8.85 (1 H, s, H_{CafC-H}), 8.52 (2 H, m, $H_{dppz10,13}$), 8.43 (1 H, m, H_{dppz7}), 8.21 (2 H, m, $H_{dppz11,12}$), 8.18 (1 H, m, H_{dppz2}), 4.29 (3 H, s, $H_{Caf7-CH3}$), 4.24 (3 H, s, $H_{Caf3-CH3}$), 3.37 (3 H, s, $H_{Caf1-CH3}$), 1.16 (3 H, s, H_{Pd-CH3}).

[(tfmdppz)Pd(Me)(Caf)][SbF$_6$]. Yield: 49% of a colourless solid. The product was found to be co-crystallised to 0.5 eq of toluene which could not be removed under reduced pressure. (Found: C, 39.94; H, 2.75; N, 11.82. Calc for $C_{28}H_{22}F_9N_8O_2PdSb{\cdot}0.5\ C_7H_8$: C, 39.92; H, 2.77; N 11.82%); δ_H(300 MHz; $(CD_3)_2CO$): 10.02 (1 H, m, H_{dppz8}), 9.88 (1 H, m, H_{dppz1}), 9.34 (1 H, m, H_{dppz6}), 8.85 (1 H, s, H_{CafC-H}), 8.82 (1 H, s, H_{dppz13}), 8.71 (1 H, m, H_{dppz10}), 8.68 (1 H, m, H_{dppz3}), 8.43 (1 H, m, H_{dppz7}), 8.37 (1 H, m, H_{dppz12}), 8.19 (1 H, m, H_{dppz2}), 4.28 (3 H, s, $H_{Caf7-CH3}$), 4.24 (3 H, s, $H_{Caf3-CH3}$), 3.36 (3 H, s, $H_{Caf1-CH3}$), 1.17 (3 H, s, H_{Pd-CH3}).

[(ndppz)Pd(Me)(Caf)][SbF$_6$]. Yield: 77% of a yellow solid. (Found: C, 36.94; H, 2.58; N, 14.41. Calc. for $C_{27}H_{22}F_6N_9O_4PdSb$: C, 36.91; H, 2.52; N, 14.35%); δ_H(300 MHz; $(CD_3)_2CO$): 10.09 (1 H, m, H_{dppz8}), 9.94 (1 H, m, H_{dppz1}), 9.38 (1 H, m, H_{dppz6}), 9.31 (1 H, s, H_{dppz10}), 8.87 (1 H, m, H_{dppz12}), 8.85 (1 H, m, H_{CafC-H}), 8.76 (1 H, m, H_{dppz13}), 8.72 (1 H, m, H_{dppz3}), 8.47 (1 H, m, H_{dppz7}), 8.22 (1 H, m, H_{dppz2}), 4.30 (3 H, s, $H_{Caf7-CH3}$), 4.25 (3 H, s, $H_{Caf3-CH3}$), 3.38 (3 H, s, $H_{Caf1-CH3}$), 1.19 (3 H, s, H_{Pd-CH3}).

[(cdppz)Pd(Me)(Caf)][SbF$_6$]. Yield: 96% of a yellow solid. (Found: C, 37.33; H, 2.45; N, 12.83. Calc. for $C_{27}H_{22}ClF_6N_8O_2PdSb$: C, 37.35; H, 2.55; N, 12.91%); δ_H(300 MHz; $(CD_3)_2CO$): 9.94 (1 H, m, H_{dppz8}), 9.80 (1 H, m, H_{dppz1}), 9.32 (1 H, m, H_{dppz6}), 8.87 (1 H, m, H_{CafC-H}), 8.67 (1 H, m, H_{dppz10}), 8.45 (3 H, m, $H_{dppz3,12,13}$), 8.15 (2 H, m, $H_{dppz2,7}$), 4.29 (3 H, s, $H_{Caf7-CH3}$), 4.26 (3 H, s, $H_{Caf3-CH3}$), 3.38 (3 H, s, $H_{Caf1-CH3}$), 1.18 (3 H, s, H_{Pd-CH3}).

[(dcdppz)Pd(Me)(Caf)][SbF$_6$]. Yield: 81% of a greenish solid. (Found: C, 35.92; H, 2.36; N, 12.42. Calc. for $C_{27}H_{21}Cl_2F_6N_8O_2PdSb$: C, 35.93; H, 2.35; N, 12.42%); δ_H(300 MHz; $(CD_3)_2CO$): 9.98 (1 H, dd, H_{dppz8}), 9.83 (1 H, dd, H_{dppz1}), 9.33 (1 H, dd, H_{dppz6}), 8.85 (1 H, s, H_{CafC-H}), 8.70 (2 H, dd, $H_{dppz10,13}$), 8.69 (1 H, dd, H_{dppz3}), 8.42 (1 H, m, H_{dppz7}), 8.17 (1 H, m, H_{dppz2}), 4.27 (3 H, s, $H_{Caf7-CH3}$), 4.23 (3 H, s, $H_{Caf3-CH3}$), 3.36 (3 H, s, $H_{Caf1-CH3}$), 1.16 (3 H, s, H_{Pd-CH3}).

General procedure for the preparation of complexes [(RR′dppz)Pd(Me)L]$^{n+}$ from [(RR′dppz)Pd(Me)Cl] (Route A)

1 eq of [(RR′dppz)Pd(Me)Cl] were solved in 20 mL of THF and stirred in the dark with 1.1 eq Ag[SbF$_6$] for 30 min. Then 1 mL CH_2Cl_2 was added and after stirring for 5 min the suspension was filtered under argon. At 0 °C the remaining solution was mixed with 1.1 eq of the desired N-ligand. The reaction mixture was stirred for 1.5 h at 0 °C and 1 h at ambient temperature. The solvent was removed under vacuum to give a solid which was washed with pentane and crystallised from acetone : pentane, 1 : 1. Products were isolated in very low yields (0.5–5.0%).

For analytical data of [(dppz)Pd(Me)(Cy)][SbF$_6$], [(dppz)-Pd(Me)(1MeCy)][SbF$_6$], [(dppz)Pd(Me)(1MeUra)] and [(dppz)-Pd(Me)(Caf)][SbF$_6$] see above. In the case of [(dppz)Pd(Me)(Py)]-[SbF$_6$] only a few yellow crystals were obtained (yield 2%). (Found: C, 40.23; H, 2.50; N, 9.74. Calc. for $C_{24}H_{18}F_6N_5PdSb$: C, 40.12; H, 2.52; N, 9.75).

Acknowledgements

We thank Dr Axel Jacobi von Wangelin, University of Cologne, for the use of the Parr-Apparatus, Dr Ingo Pantenburg and Ms. Ingrid Müller, for the collection of crystal data, Andreas O. Schüren for EPR measurements (all University of Cologne), Johnson Matthey (JM) for a generous loan of K_2PdCl_4 and the "Studienstiftung des Deutschen Volkes" for financial support (KB).

References

1 (*a*) W. Kaim, *J. Am. Chem. Soc.*, 1982, **104**, 7385–7385; (*b*) A. Juris, V. Balzani, F. Barigelletti, S. Campagna, P. Belser and A. von Zelewsky, *Coord. Chem. Rev.*, 1988, **84**, 85–277.
2 (*a*) W. Kaim, *Angew. Chem., Int. Ed. Engl.*, 1983, **22**, 171–190; (*b*) W. Kaim, *Rev. Chem. Intermed.*, 1987, **8**, 247–286.
3 (*a*) M. Atsumi, L. González and C. Daniel, *J. Photochem. Photobiol., A*, 2007, **190**, 310–320; (*b*) K. E. Erkkila, D. T. Odom and J. K. Barton, *Chem. Rev.*, 1999, **99**, 2777–2795; (*c*) X.-H. Zou and J. L.-N. Xia-Hua, *Trends Inorg. Chem.*, 2001, **7**, 99–107.
4 A. E. Friedman, J.-C. Chambron, J.-P. Sauvage, N. J. Turro and J. K. Barton, *J. Am. Chem. Soc.*, 1990, **112**, 4960–4962.
5 D. Villagra, R. López, S. A. Moya, C. Claver and A. Bastero, *Organometallics*, 2008, **27**, 1019–1021.
6 (*a*) B. M. Zeglis, V. C. Pierre and J. K. Barton, *Chem. Commun.*, 2007, 4565–4579; (*b*) J. K. Barton, *Science*, 1986, **233**, 727–734; (*c*) E. D. Stemp and J. K. Barton, Electron transfer between metal complexes bound to DNA: is DNA a wire?, in *Metal Ions in Biological Systems*, ed. A. Sigel and H. Sigel, Marcel Dekker, New York, 1996, vol. 33, pp. 325–365; (*d*) T. W. Johann and J. K. Barton, *Philos. Trans. R. Soc. London, Ser. A*, 1996, **354**, 299–324; (*e*) R. E. Holmlin, P. J. Dandliker and J. K. Barton, *Angew. Chem., Int. Ed. Engl.*, 1997, **36**, 2714–2730.
7 (*a*) N. Gupta, N. Grover, G. A. Neyhart, W. Liang, P. Singh and H. H. Thorp, *Angew. Chem., Int. Ed. Engl.*, 1992, **31**, 1048–1050; (*b*) I. Haq, P. Lincoln, D. Suh, B. Nordén, B. U. Chowdhry and J. B. Chaires, *J. Am. Chem. Soc.*, 1995, **117**, 4788–4796; (*c*) C. Turro, S. H. Bossmann, Y. Jenkins, J. K. Barton and N. J. Turro, *J. Am. Chem. Soc.*, 1995, **117**, 9026–9032; (*d*) P. Lincoln and B. Nordén, *Chem. Commun.*, 1996, 2145–2146; (*e*) P. Lincoln, A. Broo and B. Nordén, *J. Am. Chem. Soc.*, 1996, **118**, 2644–2653; (*f*) T. K. Schoch, J. L. Hubbard, C. R. Zoch, G.-B. Yi and M. Sørlie, *Inorg. Chem.*, 1996, **35**, 4383–4390; (*g*) P. Lincoln, E. Tuite and B. Nordén, *J. Am. Chem. Soc.*, 1997, **119**, 1454–1455; (*h*) E. D. A. Stemp, M. R. Arkin and J. K. Barton, *J. Am. Chem. Soc.*, 1997, **119**, 2921–2925; (*i*) C. G. Coates, L. Jacquet, J. J. McGarvey, S. E. J. Bell, A. H. R. Al-Obaidi and J. M. Kelly, *J. Am. Chem. Soc.*, 1997, **119**, 7130–7136; (*j*) R. E. Holmlin, E. D. A. Stemp and J. K. Barton, *Inorg. Chem.*, 1998, **37**, 29–34; (*k*) R. B. Nair, E. S. Teng, S. L. Kirkland and C. J. Murphy, *Inorg. Chem.*, 1998, **37**, 139–141; (*l*) P. J. Carter, C.-C. Cheng and H. H. Thorp, *J. Am. Chem. Soc.*, 1998, **120**, 632–642; (*m*) E. Amouyal, A. Homsi, J.-C. Chambron and J.-P. Sauvage, *J. Chem. Soc., Dalton Trans.*, 1990, 1841–1845; (*n*) J.-C. Chambron and J.-P. Sauvage, *Chem. Phys. Lett.*, 1991, **182**, 603–607; (*o*) J. Fees, W. Kaim, M. Moscherosch, W. Matheis, J. Klima, M. Krejcik and S. Záliš, *Inorg. Chem.*, 1993, **32**, 166–174; (*p*) E. J. C. Olson, D. Hu, A. Hörmann, A. M. Jonkman, M. R. Arkin, E. D. A. Stemp, J. K. Barton and P. F. Barbara, *J. Am. Chem. Soc.*, 1997, **119**, 11458–11467; (*q*) R. B. Nair, B. M. Cullum and C. J. Murphy, *Inorg. Chem.*, 1997, **36**, 962–965.
8 J. Fees, M. Ketterle, A. Klein, J. Fiedler and W. Kaim, *J. Chem. Soc., Dalton Trans.*, 1999, 2595–2600.

9 (*a*) R. E. Holmlin and J. K. Barton, *Inorg. Chem.*, 1995, **34**, 7–8; (*b*) R. E. Holmlin, J. A. Yao and J. K. Barton, *Inorg. Chem.*, 1999, **38**, 174–189; (*c*) R. E. Holmlin, E. D. A. Stemp and J. K. Barton, *J. Am. Chem. Soc.*, 1996, **118**, 5236–5244.

10 (*a*) V. W.-W. Yam, K. K.-W. Lo, K.-K. Cheung and R. Y.-C. Kong, *J. Chem. Soc., Dalton Trans.*, 1997, 2067–2072; (*b*) H. D. Stoeffler, N. B. Thornton, S. L. Temkin and K. S. Schanze, *J. Am. Chem. Soc.*, 1995, **117**, 7119–7128; (*c*) M. R. Waterland, K. C. Gordon, J. J. McGarvey and P. M. Jayaweera, *J. Chem. Soc., Dalton Trans.*, 1998, 609–616.

11 (*a*) M. Kato, C. Kosuge, S. Yano and M. Kimura, *Acta Crystallogr., Sect. C: Cryst. Struct. Commun.*, 1998, **C54**, 621–623; (*b*) W. Kaim and A. Klein, *Organometallics*, 1995, **14**, 1176–1186.

12 (*a*) S. Arounaguiri and B. G. Maiya, *Inorg. Chem.*, 1996, **35**, 4267–4270; (*b*) A. Klein, N. Hurkes, A. Kaiser and W. Wielandt, *Z. Anorg. Allg. Chem.*, 2007, **633**, 1659–1665.

13 C.-M. Che, M. Yang, K.-H. Wong, H.-L. Chan and W. Lam, *Chem.–Eur. J.*, 1999, **5**, 3350–3356.

14 O. A. Farus, K. P. Balashev, M. A. Ivanov, T. A. Tkacheva and A. G. Panova, *Russ. J. Gen. Chem.*, 2006, **76**, 311–316.

15 S. D. Bergman, I. Goldberg, C. Carfagna, L. Mosca and B. Milani, *Organometallics*, 2006, **25**, 6014–6018.

16 (*a*) N. Onozawa-Komatsuzaki, O. Kitao, M. Yanagida, Y. Himeda, H. Sugihara and K. Kasuga, *New J. Chem.*, 2006, **30**, 689–697; (*b*) V. W.-W. Yam, Y.-L. Pui and K.-K. Cheung, *Inorg. Chim. Acta*, 2002, **335**, 77–84; (*c*) J. Rusanova, S. Decurtins, E. Rusanov, H. Stoeckli-Evans, S. Delahaye and A. Hauser, *J. Chem. Soc., Dalton Trans.*, 2002, 4318–4320; (*d*) J. R. Schoonover, W. D. Bates and T. J. Meyer, *Inorg. Chem.*, 1995, **34**, 6421–6422; (*e*) S. Berger, J. Fiedler, R. Reinhardt and W. Kaim, *Inorg. Chem.*, 2004, **43**, 1530–1538; (*f*) J. Dyer, W. J. Blau, C. G. Coates, C. M. Creely, J. D. Gavey, M. W. George, D. C. Grills, S. Hudson, J. M. Kelly, P. Matousek, J. J. McGarvey, J. McMaster, A. W. Parker, M. Towrie and J. A. Weinstein, *Photochem. Photobiol. Sci.*, 2003, **2**, 542–554.

17 G. T. Ruiz, M. P. Juliarena, R. O. Lezna, M. R. Feliz and G. Ferraudi, *J. Photochem. Photobiol., A*, 2006, **179**, 289–297.

18 M. P. Juliarena, R. O. Lezna, M. R. Feliz, G. T. Ruiz, S. Thomas, G. Ferraudi and I. Carmichael, *J. Org. Chem.*, 2006, **71**, 2870–2873.

19 D. A. McGovern, A. Selmi, J. E. O'Brian, J. M. Kelly and C. Long, *Chem. Commun.*, 2005, 1402–1404.

20 (*a*) F. Puntoriero, S. Campagna, M. L. Di Pietro, A. Giannetto and M. Cusumano, *Photochem. Photobiol. Sci.*, 2007, **6**, 357–360; (*b*) M. Cusumano, M. L. Di Pietro and A. Giannetto, *Inorg. Chem.*, 2006, **45**, 230–235; (*c*) E. Ruba, J. R. Hart and J. K. Barton, *Inorg. Chem.*, 2004, **43**, 4570–4578; (*d*) M. Cusumano, M. L. Di Pietro, A. Giannetto, F. Nicolo, B. Nordén and P. Lincoln, *Inorg. Chem.*, 2004, **43**, 2416–2421.

21 (*a*) B. Schäfer, H. Görls, M. Presselt, M. Schmitt, J. Popp, W. Henry, J. G. Vos and S. Rau, *Dalton Trans.*, 2006, 2225–2231; (*b*) R. Ziessel, L. Bonardi and G. Ulrich, *Dalton Trans.*, 2006, 2913–2918; (*c*) T.-P. Lin, C.-Y. Chen, Y.-S. Wen and S.-S. Sun, *Inorg. Chem.*, 2007, **46**, 9201–9212.

22 M. K. Kuimova, W. Z. Alsindi, A. J. Blake, E. S. Davies, D. J. Lampus, P. Matousek, J. McMaster, A. W. Parker, M. Towrie, X.-Z. Sun, C. Wilson and M. W. George, *Inorg. Chem.*, 2008, **47**, 9857–9869.

23 S. O. Obare and C. J. Murphy, *Inorg. Chem.*, 2001, **40**, 6080–6082.

24 P. Aguirre, R. López, D. Villagra, I. Azocar-Guzman, A. J. Pardey and S. A. Moya, *Appl. Organomet. Chem.*, 2003, **17**, 36–41.

25 (*a*) Q.-X. Zhen, B.-H. Ye, J.-G. Liu, Q.-L. Zhang, L.-N. Ji and L. Wang, *Inorg. Chim. Acta*, 2000, **303**, 141–147; (*b*) Y. Liu, A. Chouai, N. N. Degtyareva, D. A. Lutterman, K. R. Dunbar and C. Turro, *J. Am. Chem. Soc.*, 2005, **127**, 10796–10797.

26 (*a*) T. Phillips, C. Rajput, L. Twyman, I. Haq and J. A. Thomas, *Chem. Commun.*, 2005, 4327–4329; (*b*) T. Phillips, I. Haq, A. J. H. M. Meijer, H. Adams, I. Soutar, L. Swanson, M. J. Sykes and J. A. Thomas, *Biochemistry*, 2004, **43**, 13657–13665.

27 F. Shao, B. Elias, W. Lu and J. K. Barton, *Inorg. Chem.*, 2007, **46**, 10187–10199.

28 A. Kleineweischede and J. Mattay, *Eur. J. Org. Chem.*, 2006, 947–957.

29 M. K. Kuimova, W. Z. Alsindi, J. Dyer, D. C. Grills, O. S. Jina, P. Matousek, A. W. Parker, P. Portius, X. Z. Sun, M. Towrie, C. Wilson, J. Yang and M. W. George, *Dalton Trans.*, 2003, 3996–4006.

30 R. E. Rülke, J. M. Ernsting, A. L. Spek, C. J. Elsevier, P. van Leeuwen and K. Vrieze, *Inorg. Chem.*, 1993, **32**, 5769–5778.

31 K. Butsch, S. Elmas, N. Sen Gupta, R. Gust, F. Heinrich, A. Klein, Y. von Mering, M. Neugebauer, I. Ott, M. Schäfer, H. Scherer and T. Schurr, *Organometallics*, 2009, **28**, 3906–3915.

32 X.-N. Li, Z.-J. Wu, Z.-J. Si, L.-Z., X.-J. Liu and H.-J. Zhang, *Phys. Chem. Chem. Phys.*, 2009, **11**, 9687–9695.

33 J. E. Huheey, E. A. Keiter, R. L. Keiter, *Inorganic Chemistry: Principles of Structure & Reactivity: Principles of Structure and Reactivity*, 1997, Prentice Hall, New Jersey.

34 J. C. Fuggle and N. Mårtensson, *J. Electron Spectrosc. Relat. Phenom.*, 1980, **21**, 275–281.

35 A. Lange, P. Tavan, D. Schröder and H. Baumgärtel, *Ber. Bunsen-Ges. Phys. Chem.*, 1981, **85**, 78–85.

36 J. V. Caspar, E. M. Kober, B. P. Sullivan and T. J. Meyer, *J. Am. Chem. Soc.*, 1982, **104**(2), 630–632.

37 A. Klein, A. Kaiser, B. Sarkar, M. Wanner and J. Fiedler, *Eur. J. Inorg. Chem.*, 2007, 965–976.

38 S. Schäfer, I. Ott, R. Gust and W. S. Sheldrick, *Eur. J. Inorg. Chem.*, 2007, 3034–3046.

39 M. Harlos, I. Ott, R. Gust, H. Alborzinia, S. Wölfl, A. Kromm and W. S. Sheldrick, *J. Med. Chem.*, 2008, **51**, 3924–3933.

40 M. A. Scharwitz, I. Ott, R. Gust, A. Kromm and W. S. Sheldrick, *J. Inorg. Biochem.*, 2008, **102**, 1623–1630.

41 R. Bieda, I. Ott, M. Dobroschke, A. Prokop, R. Gust and W. S. Sheldrick, *J. Inorg. Biochem.*, 2009, **103**, 698–708.

42 U. Schatzschneider, J. Niesel, I. Ott, R. Gust, H. Alborzinia and S. Wölfl, *ChemMedChem*, 2008, **3**, 1104–1109.

43 O. Zava, S. M. Zakkeeruddin, C. Danelon, H. Vogel, M. Grätzel and P. J. Dyson, *ChemBioChem*, 2009, **10**, 1796–1800.

44 G. M. Sheldrick, *SHELXS-97: A program for Crystal Structure Resolution*, University of Göttingen, Germany, 1997.

45 G. M. Sheldrick, *SHELXL-97: A Program for the Refinement of Crystal Structures*, University of Göttingen, Germany, 1997.

46 *STOE X-RED*, Data Reduction Program, Version 1.22/Windows, STOE & Cie, Darmstadt, 2001; *STOE X-SHAPE*, Crystal Optimisation for Numerical Absorption Correction, Version 1.06/Windows, STOE & Cie, Darmstadt, 1999.

47 (*a*) A. D. Becke, *J. Chem. Phys.*, 1993, **98**, 5648–5653; (*b*) P. J. Stephens, F. J. Devlin, C. F. Chabalowski and M. J. Frisch, *J. Phys. Chem.*, 1994, **98**, 11623–11627.

48 A. Schüter, C. Haber and R. Ahlrichs, *J. Chem. Phys.*, 1994, **100**, 5829–5836.

49 (*a*) R. Ahlrichs, M. Bär, M. Häser, H. Horn and C. Kölmel, *Chem. Phys. Lett.*, 1989, **162**, 165–169; (*b*) O. Treutler and R. Ahlrichs, *J. Chem. Phys.*, 1995, **102**, 346–354.

50 *GaussView*. Gaussian Inc., Pittsburgh PA. USA, 2000.

51 G. Schaftenaar and J. H. Noordik, *J. Comput.-Aided Mol. Des.*, 2000, **14**, 123–134.

52 L. Calucci, G. Pampaloni, C. Pinzino and A. Prescimone, *Inorg. Chim. Acta*, 2006, **359**, 3911–3920.

53 T. J. Kistenmacher, M. Rossi, J. P. Caradonna and L. G. Marzilli, *Adv. Mol. Relax. Interact. Processes*, 1979, **15**, 119–133.

